

Structure of the dengue virus envelope protein after membrane fusion

Yorgo Modis¹, Steven Ogata², David Clements² & Stephen C. Harrison¹

¹Howard Hughes Medical Institute, Children's Hospital and Harvard Medical School, 320 Longwood Avenue, Boston, Massachusetts 02115, USA

²Hawaii Biotech, Inc., 99–193 Aiea Heights Drive, Suite 200, Aiea, Hawaii, Hawaii 96701, USA

Dengue virus enters a host cell when the viral envelope glycoprotein, E, binds to a receptor and responds by conformational rearrangement to the reduced pH of an endosome. The conformational change induces fusion of viral and host-cell membranes. A three-dimensional structure of the soluble E ectodomain (sE) in its trimeric, postfusion state reveals striking differences from the dimeric, prefusion form. The elongated trimer bears three 'fusion loops' at one end, to insert into the host-cell membrane. Their structure allows us to model directly how these fusion loops interact with a lipid bilayer. The protein folds back on itself, directing its carboxy terminus towards the fusion loops. We propose a fusion mechanism driven by essentially irreversible conformational changes in E and facilitated by fusion-loop insertion into the outer bilayer leaflet. Specific features of the folded-back structure suggest strategies for inhibiting flavivirus entry.

Membrane fusion is the central molecular event during the entry of enveloped viruses into cells. The critical agents of this process are viral surface proteins, primed to facilitate bilayer fusion and triggered to do so by the conditions of viral interaction with the target cell. The best-studied example is the influenza virus haemagglutinin (HA), synthesized as a single-chain precursor and then cleaved into two chains, known as HA₁ and HA₂, during transport of the trimeric glycoprotein to the cell surface. The binding of HA₁ to a cell-surface receptor leads to endocytic uptake; acidification of the endosome triggers dramatic conformational rearrangement of HA₂. The latter is a two-stage process. Exposure of the amino-terminal 'fusion peptide' of HA₂ first allows it to insert into the endosomal membrane; subsequent folding-over of the entire HA₂ polypeptide chain brings together its N and C termini and thus forces the target-cell membrane (held by the fusion peptide) and the viral membrane (held by the C-terminal transmembrane anchor of HA) against each other.

HA is the prototype of a large class of viral fusion proteins—for example, those of other myxo- and paramyxoviruses such as measles virus, retroviruses such as HIV, and filoviruses such as Ebola virus (reviewed in ref. 1). All of these 'class I' viral fusion proteins are two-

chain products of a cleaved, single-chain precursor, and all bear a hydrophobic fusion peptide at or near the N terminus created by the cleavage². Moreover, in all class I fusion proteins, a three-chain, α -helical, coiled-coil assembles during the conformational change, drives the fusion peptide towards the target-cell membrane^{3–5}, and creates the central structural element of the fusion machinery^{6,7}.

An architecturally and evolutionarily distinct class of fusion proteins is found on flaviviruses, such as yellow fever, West Nile, and dengue viruses, and on alphaviruses, such as Semliki Forest and Sindbis viruses. These proteins associate with a second, 'protector' protein, the cleavage of which primes the fusion protein to respond to acidic pH. The fusion protein is called E in flaviviruses and E1 in alphaviruses. Structures have been determined for the ectodomains of three class II proteins in their prefusion states^{8–10}. Those of two flaviviruses, tick-borne encephalitis (TBE) and dengue viruses, are dimeric, both in solution¹¹ and on the viral membrane surface^{12,13} (Fig. 1). They have three domains, with folds based largely on β -sheets. One of these (domain II), an elongated, finger-like structure, bears a loop at its tip with a hydrophobic sequence conserved among all flaviviruses. Experiments with TBE virus show that this 'cd loop' (residues 98–109 in dengue type 2) is

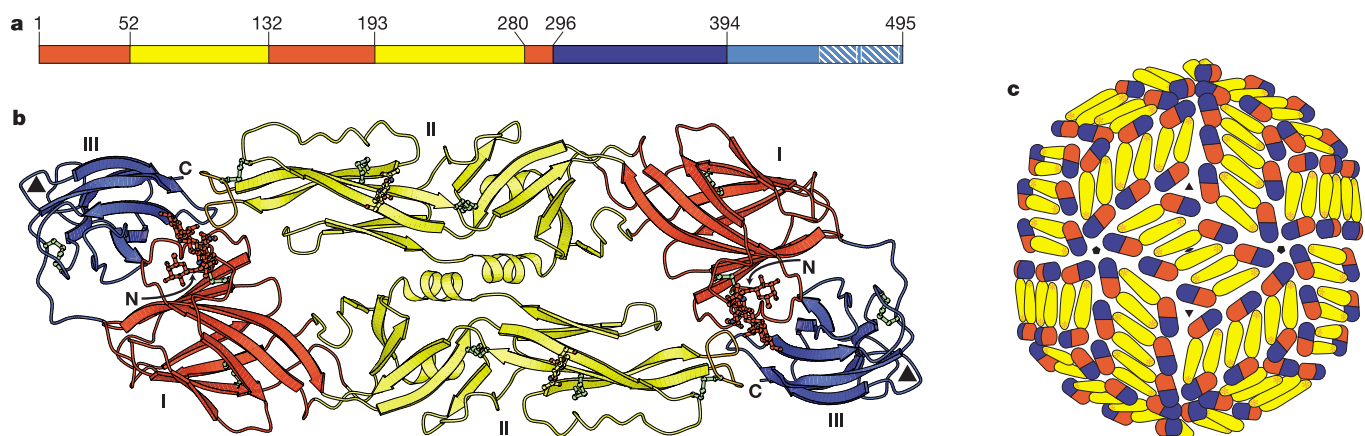


Figure 1 Structure of the dimer of dengue E soluble fragment (sE) in the mature virus particle. **a**, The three domains of dengue sE. Domain I is red, domain II is yellow, domain III is blue. A 53-residue 'stem' segment links the stably folded sE fragment with the C-terminal transmembrane anchor. **b**, The sE dimer¹⁰. This is the conformation of E in the

mature virus particle and in solution above the fusion pH. **c**, Packing of E on the surface of the virus. Electron cryomicroscopy image reconstructions show that 90 E dimers pack in an icosahedral lattice¹³.

responsible for attachment of soluble E ectodomains to target membranes and that the hydrophobic residues are essential for its activity¹⁴. These and other data, including results from studies of alphaviruses^{15,16}, which have a very similar cd-loop structure, support the view that the cd loop of class II fusion proteins has a function analogous to that of the N-terminal fusion peptide in class I fusion proteins: insertion into the host-cell membrane and provision of an attachment point for drawing host-cell and viral membranes together¹. We refer to the cd loop as the ‘fusion loop’, reserving ‘fusion peptide’ for the N-terminal segment of class I fusion proteins.

An important missing link in our picture of membrane fusion is a direct view of a fusion peptide or loop as it inserts into a target membrane. The crystal structure we describe here—of the soluble ectodomain of dengue virus type 2 E protein (sE) in its trimeric, postfusion conformation—provides such a link. The fusion loops of the three subunits come together to form a membrane-insertable, ‘aromatic anchor’ at the tip of the trimer. The fusion loop retains its prefusion conformation. Neighbouring hydrophilic groups restrict insertion to the proximal part of the outer lipid-bilayer leaflet. The entire ectodomain of the protein folds back on itself, directing the C-terminal, viral membrane anchor towards the fusion loop. Comparison with the prefusion structure of the same protein¹⁰ allows us to propose a mechanism for fusion driven by an essentially irreversible conformational change in the protein and assisted by membrane distortions imposed by fusion-loop insertion. Specific features of the folded-back structure suggest strategies for inhibiting flavivirus entry. The postfusion structure of an alphavirus fusion protein¹⁷ described in the accompanying paper shows an analogous conformation and leads to similar conclusions.

Membrane insertion and trimer formation

Like its TBE homologue, the dimer formed by dengue sE (residues 1–395 of E) dissociates reversibly^{10,11}. At acidic pH, dissociation is essentially complete at protein concentrations of 1 mg ml⁻¹; at neutral pH, the dissociation constant is one to two orders of magnitude smaller. The fusion loop at the tip of domain II would be exposed in the monomer^{8,10}, but exposure does not cause non-specific aggregation of the protein¹¹. Liposome coflotation experiments show that the fusion loop of monomeric TBE sE allows association with lipid membranes and that this membrane association catalyses irreversible formation of sE trimers at low pH¹⁸. Dengue E exhibits an identical behaviour: on acidification, sE dimers dissociate, bind liposomes and trimerize (see Methods). Membrane-associated sE is readily detected by electron microscopy of negatively stained preparations (Fig. 2a); chemical cross-linking confirms that the protein has trimerized (Fig. 2b). The trimers are tapered rods, about 70–80 Å long and 30–50 Å in diameter, with the long axis perpendicular to the membrane and their wide end distal to it. They tend to cluster on the liposome surface, often forming a continuous layer. These heavily decorated areas appear to have a greater than average membrane curvature, resulting in smaller vesicles (Fig. 2a). This observation suggests that E trimers can induce curvature, a property that may help promote fusion (see below). The dengue sE trimers can be solubilized with the detergent *n*-octyl-β-D-glucoside (β-OG); they remain trimeric at all pH values between 5 and 9, as determined by gel filtration chromatography (data not shown).

Domain rearrangements in the trimer

Crystals of the detergent-solubilized dengue sE trimers diffract to high resolution (2.0 Å); the structure was determined by molecular replacement (see Methods). The three domains of sE retain most of their folded structures, but undergo major rearrangements in their relative orientations, through flexion of the interdomain linkers (Fig. 3). Domain II rotates approximately 30° with respect to domain I, about a hinge near residue 191 and the kl hairpin

(residues 270–279), where mutations that affect the pH threshold of fusion are concentrated¹⁰. As a result of the rotation, the base of the kl hairpin is pulled apart, and the l strand forms a new set of hydrogen bonds with the D₀ strand of domain I, shifted by two residues from the hydrogen-bonding pattern in the dimer¹⁰. Although detergent is present, the kl hairpin does not adopt the open conformation seen in the dimer with bound β-OG¹⁰. The small hydrophobic core beneath this hairpin acts as a ‘greased hinge’ for the rotation between domains I and II.

Domain III undergoes the most significant displacement in the dimer-to-trimer transition. It rotates by about 70°, and its centre of mass shifts by 36 Å towards domain II. This folding-over brings the C terminus of domain III (residue 395) 39 Å closer to the fusion loop.

Changes in the secondary structure

The 10-residue linker between domains I and III accommodates their large relative displacement during trimer formation. The linker, which has a poorly ordered, extended structure in the prefusion dimer¹⁰ (Fig. 3a), inserts in as a short β-strand between strands A₀ and C₀ in domain I (Fig. 3b). As part of this rearrangement, the C-terminal region of A₀ peels away from C₀ and switches to the other β-sheet, thereby creating the surface for an annular trimer contact with the two other A₀ strands in the trimer.

The transition to the trimer state is irreversible. The refoldings just described may impart irreversibility by contributing a high barrier to initiation of trimerization (sE monomers do not trimerize at low pH without liposomes) and an even higher barrier to dissociation of trimers once they have formed.

Trimer contacts

Dengue E trimers assemble through both polar and nonpolar contacts in four areas: at the membrane-distal end of the trimer, at the base of domain II, at the tip of domain II, and at the packing interface between domains I and III (Fig. 4). The total surface buried per monomer during trimer assembly is 3,900 Å²—twice the 1,950 Å² per monomer buried in the dimer. An additional 1,035 Å² are buried within each monomer during the domain rearrangements observed in our structure. These numbers help to explain why trimers are much more stable than dimers in solution.

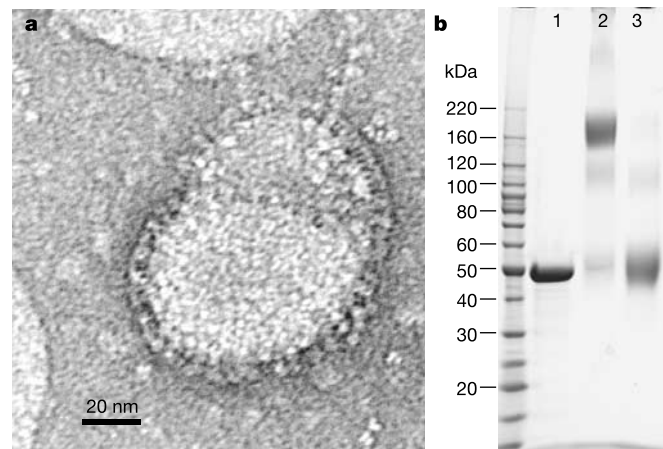


Figure 2 Trimer formation and membrane insertion of dengue E protein. **a**, Electron micrograph showing E trimers inserted into liposomes. The liposomes are heavily decorated with E trimers. A large portion of the trimer can be seen protruding from the membrane. The samples were stained with uranyl formate (see Methods). **b**, E trimers can be covalently cross-linked with ethylene glycol bis-succinimidyl-succinate (EGS) after insertion into liposomes. Lane 1, E solubilized from liposomes at pH 5.5 and not cross-linked. Lane 2, E solubilized from liposomes at pH 5.5 and cross-linked with EGS. Lane 3, E cross-linked with EGS at pH 7 in the absence of lipid.

They also help to account for the irreversibility of the fusion-activating conformational change. Additional trimer contacts are likely to be contributed by the stems, as described below.

An extended cavity, which runs along the three-fold axis, separates the trimer contact areas at the top and at the base of domain II. A narrow opening connects this cavity with the exterior solvent, but it may be occluded by the stem in the full-length protein (Fig. 4b). An anion, modelled as a chloride ion, lies on the three-fold axis near the tip of domain II. It is liganded by three amide nitrogens (from Lys 110 of each subunit) and three water molecules. Between this anion and the domain II tip, a small hydrophobic core underpins the nonpolar, bowl-shaped apex formed by the three clustered fusion loops (Fig. 4e).

The fusion loop

The fusion loops in the sE trimer have the same conformation as in the dimer¹⁰. Because the trimers are obtained by detergent extraction from liposomes, we conclude that this conformation is also present when the loop inserts into a membrane. Furthermore, because dimers can dissociate reversibly, the fusion loop is stable when fully exposed. It thus appears that the fusion loop retains essentially the same conformation, whether buried against another subunit, inserted into a lipid membrane, or exposed to aqueous solvent.

In the trimer, the three hydrophobic residues in the fusion loop conserved among all flaviviruses—Trp 101, Leu 107 and Phe 108—are fully exposed on the molecular surface, near the three-fold axis. They form a bowl-like concavity at the trimer tip, with a hydrophobic rim (Fig. 4e). There are no lipid or detergent molecules visible in the electron density near the fusion loop in either of our crystal forms (see Methods). Indeed, in the P321 crystal form, there can be no detergent micelle covering the fusion loop, as this region is involved in close crystal contacts with residues in domain III of a symmetry-related molecule. We conclude that detergent is required to dissolve away the liposome on which the trimer formed, and hence to solubilize the protein, but that once the protein has been extracted from the membrane, the three-fold-clustered fusion loops do not retain a tightly associated detergent micelle.

How deeply, then, do fusion loops penetrate into the membrane? Tryptophans tend to appear in membrane proteins at the interface between the hydrocarbon and head-group layers of the lipid¹⁹, but if the indole amine participates in a hydrogen bond, as is the case for Trp 101, the side chain may be completely buried in the hydrocarbon layer. We therefore propose that the E trimers penetrate about 6 Å into the hydrocarbon layer of the target membrane. They cannot penetrate further, because of exposed carbonyls and charged residues on the outside rim of the fusion-loop bowl (Fig. 4e). Thus, the fusion loop is held in the membrane mainly by an 'aromatic

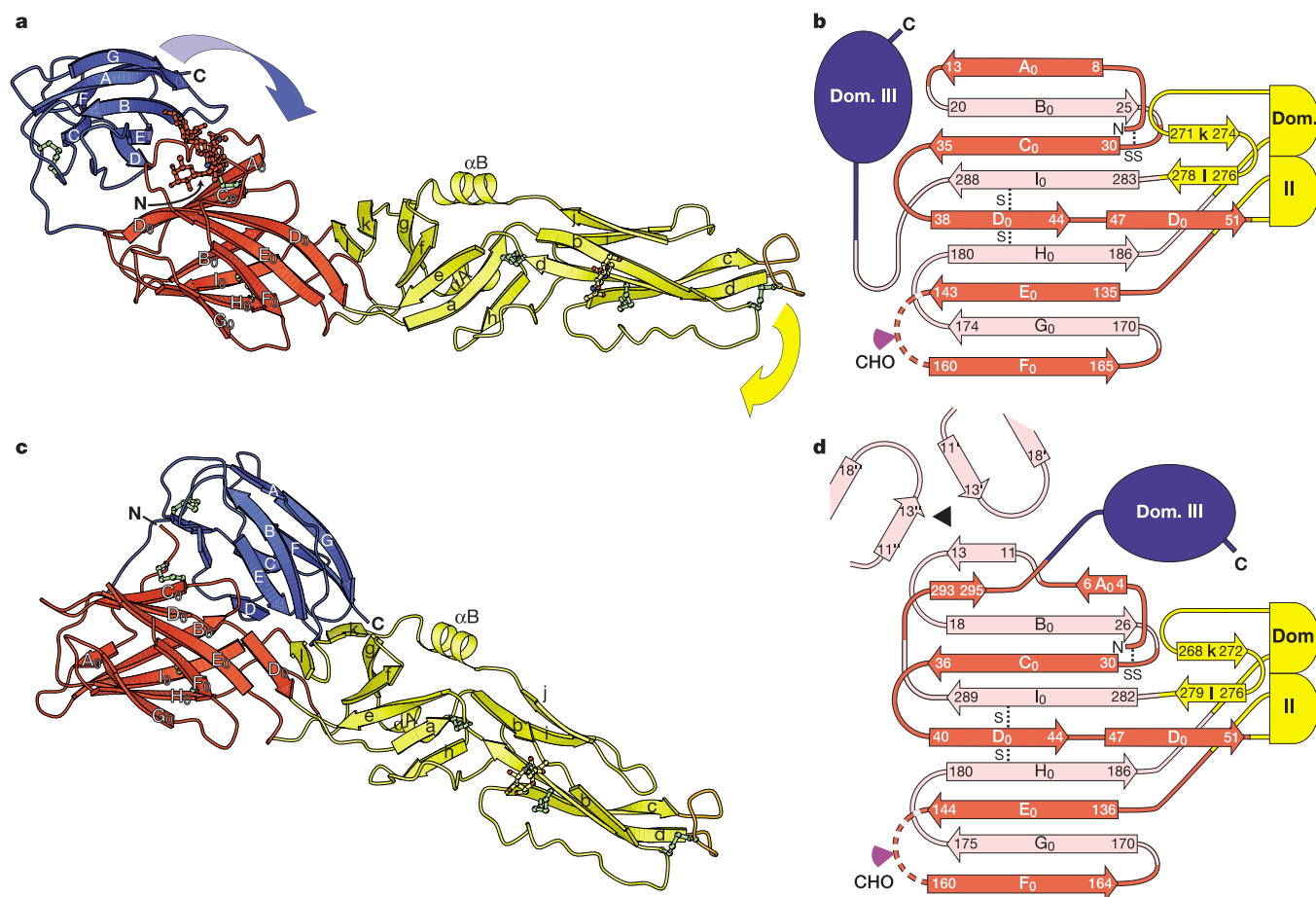


Figure 3 Domain rearrangements in the dengue sE monomer during the transition to trimer. **a**, An sE monomer in its prefusion conformation. This is the structure adopted in mature virus particles and in solution at pH > 7, when sE is a dimer. **b**, Schematic representation of the secondary structure of domain I and links to domains II and III in the prefusion conformation. **c**, An sE monomer in its postfusion conformation, as seen in sE trimers. The three domains have rotated and shifted with respect to each other, bringing

the C terminus 39 Å closer to the fusion loop (orange). The fusion loop retains essentially the same conformation before and after fusion. **d**, Secondary structure of domain I and its links to domains II and III in the trimeric, postfusion conformation. The domain I–III linker inserts between strands A₀ and C₀. The C-terminal region of A₀ flips out, switches to the other β-sheet, and creates an annular trimer contact with the two other A₀ strands in the trimer.

anchor' formed by Trp 101 and Phe 108. The bowl is lined by the hydrophobic side chains of Leu 107 and Phe 108, so that it cannot accommodate lipid headgroups. We expect that fatty-acid chains from the inner leaflet of the membrane may extend across to contact the base of the fusion-loop bowl, or that fatty-acid chains from the outer leaflet may bend over to fill it. In either case, insertion will produce a distortion in the bilayer, which could be important for the fusion process (see below).

A postfusion conformation

The folding back of domain III and the rearrangement of β -strands at the trimer interface projects the C terminus of sE towards the fusion loop, and positions it at the entrance of a channel, which extends towards the fusion loops along the intersubunit contact

between domains II (Fig. 4a, b). The 53-residue 'stem' connecting the end of the sE fragment with the viral transmembrane anchor could easily span the length of this channel, even if the stem were entirely α -helical. By binding in the channel, the stem would contribute additional trimer contacts with domain II of another subunit (Fig. 4b). The stem does indeed promote trimer assembly even in the absence of liposomes²⁰. In the virion, the stem forms two α -helical segments, which lie near the outer surface of the lipid bilayer and contact the subunit from which they emanate²¹. The proposed stem conformation places the viral transmembrane domain in the immediate vicinity of the fusion loop, just as in the postfusion conformations of class I viral fusion proteins. We therefore believe that the trimer we have crystallized represents a postfusion state of the protein.

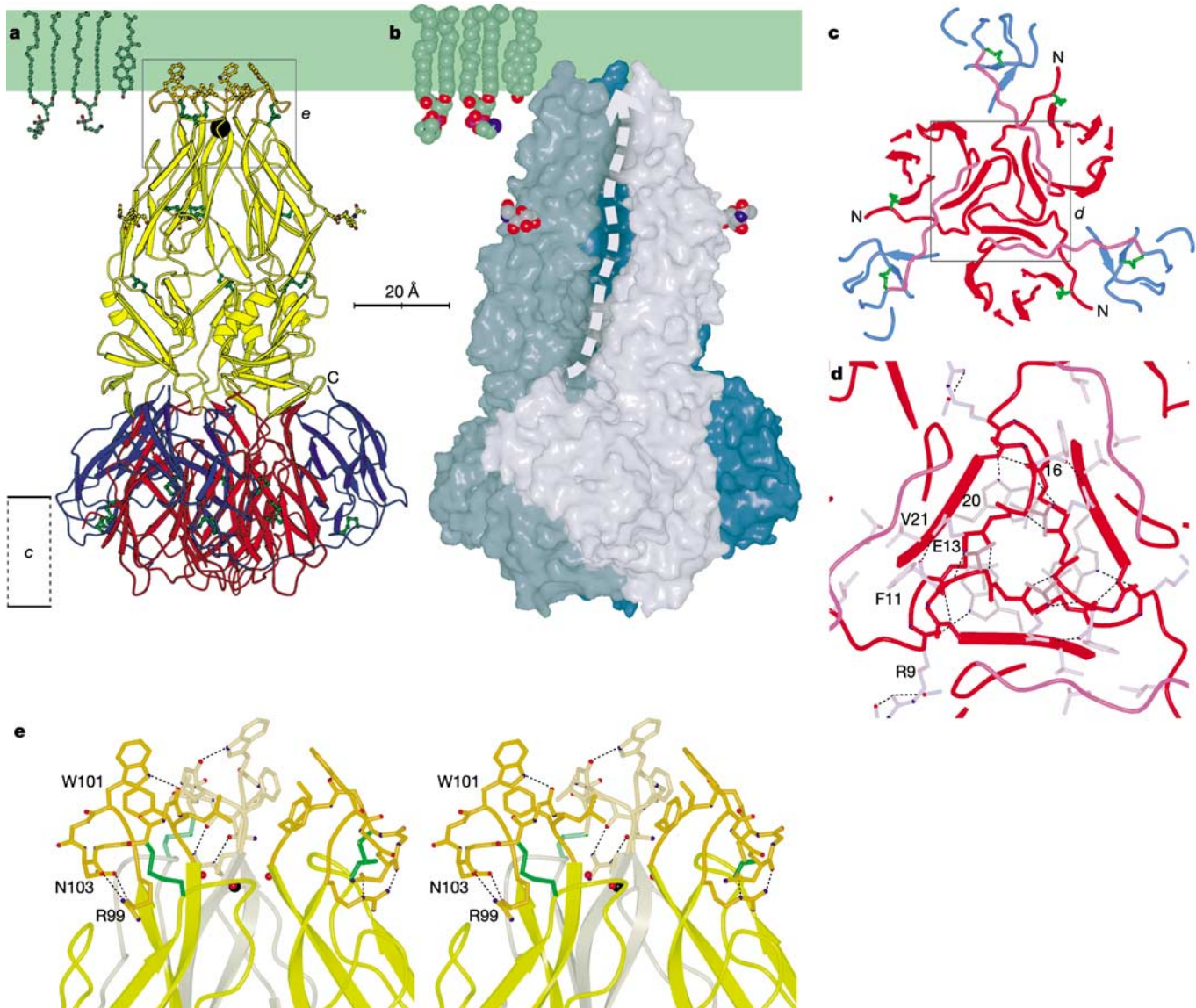


Figure 4 The dengue sE trimer. **a**, Ribbon diagram coloured as in Fig. 1b. Hydrophobic residues in the fusion loop (orange) are exposed. The expected position of the hydrocarbon layer of the fused membrane is shown in green. Representative lipids are shown to scale. A chloride ion (black sphere) binds near the fusion loop. **b**, Surface representation of the trimer. The dashed grey arrow indicates the most likely location for the stem (see text). An extended cavity is visible near the tip of the trimer; access to this cavity will probably be occluded by the stem. The glycan on Asn 67 and representative lipids are shown in space-filling representation. **c**, The membrane-distal end of the trimer,

where most trimer contacts are formed. The view is along the three-fold axis. **d**, Close-up of **c** showing trimer contacts. The A_0B_0 loop forms an annular trimer contact. The domain I–III linker (purple) adopts an extended conformation and forms additional trimer contacts. **e**, Close-up of the aromatic anchor formed by Trp 101 and Phe 108, in the fusion loop (orange). The three clustered fusion loops form a nonpolar, bowl-shaped apex, which is underpinned by a small hydrophobic core. Underneath, a chloride ion (black sphere) forms a trimer contact.

Mechanism of membrane fusion

The structure described here, combined with previous knowledge, allows us to propose the following mechanism for how conformational changes in the flavivirus E protein promote membrane fusion.

(1) E associates with a cell-surface receptor, probably through domain III^{22–28} (Fig. 5a); there is evidence for glycan-mediated interactions as well^{29–31}. Receptor binding leads to endosomal uptake.

(2) Reduced pH in the endosome causes E dimers on the virion surface to dissociate³², exposing their fusion loops and allowing domains I and II to flex relative to one another (Fig. 5b). Evidence for a pH-dependent hinge at the domain I–domain II interface includes the location of mutations that alter the pH threshold of fusion¹⁰, as well as the difference in orientation between the pre- and postfusion structures. Release of constraints imposed by dimer contacts may also allow the stem to extend away from the membrane. Some combination of these two sources of flexibility permits domain II to turn outward, away from the virion surface, and to insert its fusion loop into the target-cell membrane.

(3) Outward projection of domain II will destroy tight packing interactions on the virion outer surface, allowing lateral rearrangement of E monomers. Thus, the absence of trimer clustering in the virion¹³ is not, in principle, a barrier to trimer formation. Target membranes probably catalyse trimerization¹⁸, leading to a prefusion intermediate, in which the trimer bridges host-cell and viral membranes, with its fusion loops bound to the former and its transmembrane tail anchored in the latter (Fig. 5c). This species is analogous to the ‘prehairpin’ intermediate postulated for class I viral fusion mechanisms³³.

(4) Formation of trimer contacts spreads from the fusion loops at the trimer tip to domain I at the base. Domain III shifts and rotates, folding the C terminus of sE back towards the fusion loop (Fig. 5d). The length of the interdomain linker permits independent rotation of individual domains III, allowing for the spontaneous symmetry-breaking required at this point. Cooperativity and irreversibility occur only when the exchange of β -strands shown in Fig. 3d locks in

the final trimer interaction of domain I and the final folded-back position of domain III. Free energy released by this refolding can drive the two membranes to bend towards each other^{3–5}, forming apposing ‘nipples’³⁴ (Fig. 5d). Positive bilayer curvature induced by fusion-loop insertion might stabilize the lateral surfaces of such protrusions. A ring of trimers may be needed properly to deform the membrane. We cannot yet specify the number of trimers in such a ring nor how their conformational changes are coupled. It is possible that coupling is provided simply by the resistance of the membranes to deformation: only when several trimers act in concert can folding back reach the barrier of β -strand exchange.

(5) Formation of a ‘hemifusion stalk’, with proximal leaflets fused and distal leaflets unfused (Fig. 5e), is thought to be an essential intermediate in the membrane fusion reaction^{34–36}. Hemifusion could occur at any point during the conformational changes represented in Fig. 5d and e, depending on the length of the hemifusion stalk. We suggest that hemifusion would happen following the β -strand exchange step that locks domains III into their trimer positions. It must precede final zippering up of the stems, as full pore formation must occur before the transmembrane segments can reach their probable final positions around the periphery of the fusion loops. Hemifusion stalks can ‘flicker’ open into narrow fusion pores³⁵. Migration of the transmembrane segments along a transient pore will prevent its closing. Thus, if the transmembrane segments or adjacent stem regions ‘snap’ into place around the tips of domains II, formation of the symmetrical final structure (Fig. 5f) could drive the transition from stalk to pore.

(6) In the final state, the trimer has reached the conformation seen in our crystal structure, with the stems (not present in our current crystals) docked along the surface of domains II and with the fusion loops and transmembrane anchors now next to each other in the fused membrane (Fig. 5f).

Comparison with class I fusion

Class I and class II viral fusion proteins clearly have some common mechanistic features (Fig. 5). The most striking of these is a folding back of the protein during the fusion transitions, so that its two membrane attachment points come together in the postfusion structure. Class I proteins fold back by zippering up an ‘outer layer’ (at least partly α -helical) around a central, trimeric coiled-coil¹. Our structure of trimeric dengue sE shows that class II proteins do so by nucleating trimer formation around an elongated, finger-like fusion domain, by rearranging two other domains, and (probably) by zippering an extended C-terminal stem along the trimer surface.

Class II viral fusion proteins form trimers from monomers (dissociated homodimers in the case of flaviviruses; dissociated heterodimers in the case of alphaviruses³⁷), while class I proteins are trimeric in their prefusion state². But comparison of the pre- and postfusion states of influenza haemagglutinin—the only previous case where both structures are known for the same protein—shows that most of the trimer contacts in the latter state are not present in the former⁶. That is, just as in the trimerization of dengue E, the important trimer interactions in the final state form during the transition. These contacts are close to the three-fold axis, and they must be present before zippering up of an outer layer can occur. Indeed, the postulated prefusion intermediate is, both for class I fusion proteins and now for class II, a structure in which these central trimer contacts have formed but the zippering-up of the outer layer has not yet begun (Fig. 5).

Is our structure for the membrane-inserted state of the flavivirus fusion loops relevant also for class I fusion-peptide insertion? An NMR structure of an isolated, 20-residue influenza virus A fusion peptide associated with a detergent micelle suggests a slightly kinked α -helix, with its N and C termini embedded in the outer leaflet and the kink (at about residue 10) on the surface³⁸. Unlike the flavivirus and alphavirus fusion loops, however, the class-I fusion peptides

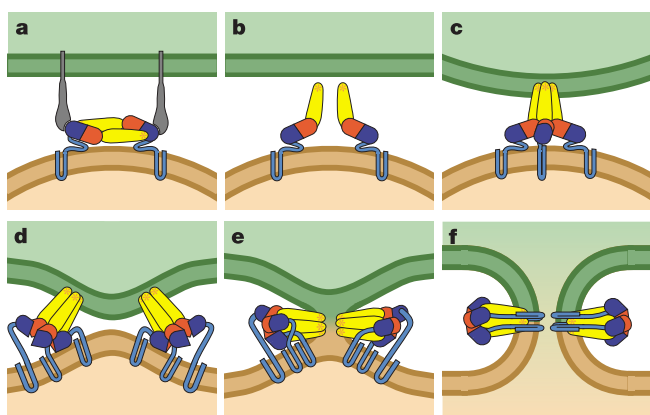


Figure 5 Proposed mechanism for fusion mediated by class II viral fusion proteins. Full-length E is represented as in Fig. 1c, with the stem and viral transmembrane anchor in cyan. **a**, E binds to a receptor on the cell surface and the virion is internalized to an endosome. **b**, Reduced pH in the endosome causes domain II to hinge outward from the virion surface, exposing the fusion loop, and allowing E monomers to rearrange laterally in the plane of the viral membrane. **c**, The fusion loop inserts into the hydrocarbon layer of the host-cell membrane, promoting trimer formation. **d**, Formation of trimer contacts spreads from the fusion loop at the tip of the trimer, to the base of the trimer. Domain III shifts and rotates to create trimer contacts, causing the C-terminal portion of E to fold back towards the fusion loop. Energy release by this refolding bends the apposed membranes. **e**, Creation of additional trimer contacts between the stem-anchor and domain II leads first to hemifusion and then (**f**) to formation of a lipidic fusion pore.

have no particular sequence conservation. Indeed, the Ebola virus fusion peptide begins at the 23rd residue of GP2, rather than at the N terminus³⁹, and a cysteine preceding the fusion peptide probably makes a disulphide bond with a cysteine C terminal to it. Thus, whatever its conformation, this peptide must enter and leave the membrane from the external face. The available data for class I fusion peptides are thus consistent with one important feature of our structure and of the SFV E1 postfusion structure¹⁷: insertion only into the outer bilayer leaflet.

Insertion only into the outer leaflet is also consistent with the requirement of a complete C-terminal transmembrane anchor on influenza HA or Simian virus 5 for full fusion to take place^{40–42}. Indeed, as illustrated by Fig. 5f, one of the two membrane attachment structures must span the bilayer to stabilize a fusion pore. This appears to be the C-terminal anchor for both class I and class II fusion.

Strategies for inhibiting flavivirus fusion

The discovery of a hydrophobic ligand-binding pocket beneath the kl loop in the prefusion structure of dengue sE has suggested one possible strategy for inhibiting flavivirus entry: by interfering with the fusion transition¹⁰. The rationale for that proposal is enhanced by our new structure, which shows that significant rearrangements do occur around the kl loop during the conformational change. The trimer structure also suggests a second strategy for interfering with fusion, related to an approach successful in developing an HIV antiviral compound⁴³. Peptides corresponding to the C-terminal region of the gp41 ectodomain inhibit HIV-1 entry, probably by binding to the trimeric, N-terminal ‘inner core’ of the protein and interfering with the folding back against it of the C-terminal ‘outer layer’⁴⁴. An analogous strategy may be successful with class II viral fusion proteins, such as those of dengue and perhaps of hepatitis C. The way in which the stem is likely to fold back suggests that peptides derived from stem sequences could block completion of the conformational change, by interacting with surfaces on the clustered domains II. This would interfere with the final stage of the conformational change, whereas targeting the pocket beneath the kl loop would interfere with the first stage. Inhibitors developed from these two strategies could thus act in synergy. □

Methods

Expression and purification of dengue sE

Soluble E protein (sE) from dengue virus type 2 S1 strain⁴⁵ was supplied by Hawaii Biotech. The protein was expressed in *Drosophila melanogaster* Schneider 2 cells (obtained from ATCC) using a pMtt vector (GlaxoSmithKline) containing the dengue 2 prM and E genes (nucleotides 539–2121), as previously described⁴⁶. The resulting prM–E preprotein is processed during secretion to yield sE, which was purified from the cell culture medium by immunoaffinity chromatography⁴⁷.

Preparation of dengue sE trimers

Dengue sE trimers were obtained as follows, based on a method developed for TBE virus sE¹⁸. 1-palmitoyl-2-oleoyl-sn-glycero-3-phosphocholine, 1-palmitoyl-2-oleoyl-sn-glycero-3-phosphoethanolamine (Avanti Polar Lipids) and 1-cholesterol (Sigma) were dissolved in chloroform, mixed in a 1:1:1 molar ratio, and dried under high vacuum for over 4 h. The lipid film was resuspended in 10 mM triethanolamine (TEA) of pH 8.3, 0.14 M NaCl and subjected to five cycles of freeze-thawing, followed by 21 cycles of extrusion through two 0.2 µm polycarbonate filter membranes (Whatman). Purified sE was added in a 1:680 protein:lipid molar ratio and incubated at 37 °C for 5 min. The pH was lowered to endosomal levels by adding 75 mM MES of pH 5.4, and the protein was incubated at 37 °C for 30 min. Liposomes were solubilized with a 20-fold molar excess of *n*-octyl-β-D-glucoside (β-OG) and 4 mM *n*-undecyl-β-D-maltoside (UDM) (Anatrace). Excess lipid was removed by cation exchange chromatography with MonoS (Pharmacia) in 25 mM citric acid of pH 5.26, 70 mM NaCl, 4 mM UDM. After washing with 0.4 M NaCl, the protein was eluted with 1–1.5 M NaCl. E trimers were further purified by gel filtration on a Superdex 200 column (Pharmacia) in 8 mM TEA of pH 7, 80 mM NaCl, 3 mM UDM. The sE trimers were concentrated to about 15 mg ml⁻¹ for crystallization and dialysed against the gel filtration buffer using a 50-kDa molecular-mass cutoff membrane (Spectrapor).

Crystallization and data collection

Crystals were grown at 20 °C by hanging-drop vapour diffusion by mixing equal volumes of protein solution and the following reservoir solution: 20–30% polyethylene glycol 400

(PEG400), 0.1 M MOPS pH 7–8 or Tris pH 8–9, 80 mM NaCl. Two crystal forms were obtained: plates of space group *P321* with cell dimensions $a = b = 76.2 \text{ \AA}$, $c = 131 \text{ \AA}$, and rhomboids of space group *P3₁21* with cell dimensions $a = b = 153 \text{ \AA}$, $c = 143 \text{ \AA}$. The asymmetric unit of the *P321* crystals contains one molecule of sE; that of the *P3₁21* crystals, one trimer (three molecules) of sE. Cryoprotection was achieved by raising the concentration of PEG400 to 30%. Crystals were frozen in liquid nitrogen, and all data were collected at 100 K on BioCARS beamline 14-BM-C at the Advanced Photon Source (Argonne National Laboratory). The data were processed with HKL⁴⁸. Data collection statistics are presented in Supplementary Table 1.

Chemical cross-linking

sE was covalently cross-linked with ethylene glycol *bis*-(succinimidyl succinate) (EGS). 10 µM–1 mM EGS was added from a fresh 0.1 M stock solution in dimethyl sulphoxide to about 5 µg E at 10 µg ml⁻¹. Acidic solutions were neutralized with TEA of pH 8.5. After 30 min at room temperature, EGS was quenched with 20 mM Tris for 15 min. Protein was precipitated with trichloroacetic acid and resuspended in SDS–polyacrylamide gel electrophoresis (PAGE) sample buffer for gel electrophoresis.

Electron microscopy

Dengue sE trimers inserted into liposomes were prepared as described above and adsorbed to glow-discharged, carbon-coated copper grids. Samples were washed with two drops of deionized water, stained with two drops of 0.7% uranyl formate for 20 s, washed with water, and blotted gently. Micrographs were recorded on a Philips Tecnai 12 electron microscope at 100 kV and 64,000-fold magnification.

Structure determination

The crystal structure of dengue E in the postfusion conformation was determined by molecular replacement using individual domains from the prefusion dengue E structure¹⁰ (Protein Data Bank code 1OKE) as search models, and the *P321* data set (see Supplementary Table 1). Domain II was placed first, followed by domain I, with AmoRe⁴⁹. Domain III was placed last, with CNS⁵⁰. The atomic coordinates of the three domains were refined as rigid bodies. The model was rebuilt with O⁵¹ based on $2F_o - F_c$ and $F_o - F_c$ Fourier maps. Residues 1–17, 34–40, 49–54, 128–137, 165–192, 290–299 and 341–346 were built *de novo*. Coordinates were then refined against data up to 2.0 Å resolution by simulated annealing using torsion-angle dynamics with CNS⁵⁰, and rebuilt with O, in iterative cycles. Later cycles included restrained refinement of B-factors for individual atoms and energy minimization against maximum likelihood targets with CNS. The final model contains residues 1–144 and 159–394, an *n*-acetyl glucosamine glycan on residue 67, 205 water molecules and one chloride ion. Residues 145–158 and the glycan on residue 153 are disordered. Refinement statistics are presented in Supplementary Table 1.

Received 16 August; accepted 24 October 2003; doi:10.1038/nature02165.

1. Skehel, J. J. & Wiley, D. C. Receptor binding and membrane fusion in virus entry: the influenza haemagglutinin. *Annu. Rev. Biochem.* **69**, 531–569 (2000).
2. Wilson, I. A., Skehel, J. J. & Wiley, D. C. Structure of the haemagglutinin membrane glycoprotein of influenza virus at 3 Å resolution. *Nature* **289**, 366–373 (1981).
3. Baker, K. A., Dutch, R. E., Lamb, R. A. & Jardetzky, T. S. Structural basis for paramyxovirus-mediated membrane fusion. *Mol. Cell* **3**, 309–319 (1999).
4. Melikyan, G. B. *et al.* Evidence that the transition of HIV-1 gp41 into a six-helix bundle, not the bundle configuration, induces membrane fusion. *J. Cell Biol.* **151**, 413–423 (2000).
5. Russell, C. J., Jardetzky, T. S. & Lamb, R. A. Membrane fusion machines of paramyxoviruses: capture of intermediates of fusion. *EMBO J.* **20**, 4024–4034 (2001).
6. Bullough, P. A., Hughson, F. M., Skehel, J. J. & Wiley, D. C. Structure of influenza haemagglutinin at the pH of membrane fusion. *Nature* **371**, 37–43 (1994).
7. Chen, J., Skehel, J. J. & Wiley, D. C. N- and C-terminal residues combine in the fusion-pH influenza haemagglutinin HA(2) subunit to form an N cap that terminates the triple-stranded coiled coil. *Proc. Natl Acad. Sci. USA* **96**, 8967–8972 (1999).
8. Rey, F. A., Heinz, F. X., Mandl, C., Kunz, C. & Harrison, S. C. The envelope glycoprotein from tick-borne encephalitis virus at 2 Å resolution. *Nature* **375**, 291–298 (1995).
9. Lescar, J. *et al.* The fusion glycoprotein shell of Semliki Forest virus: an icosahedral assembly primed for fusogenic activation at endosomal pH. *Cell* **105**, 137–148 (2001).
10. Modis, Y., Ogata, S., Clements, D. & Harrison, S. C. A ligand-binding pocket in the dengue virus envelope glycoprotein. *Proc. Natl Acad. Sci. USA* **100**, 6986–6991 (2003).
11. Allison, S. L. *et al.* Oligomeric rearrangement of tick-borne encephalitis virus envelope proteins induced by an acidic pH. *J. Virol.* **69**, 695–700 (1995).
12. Ferlenghi, I. *et al.* Molecular organization of a recombinant subviral particle from tick-borne encephalitis virus. *Mol. Cell* **7**, 593–602 (2001).
13. Kuhn, R. J. *et al.* Structure of dengue virus: implications for flavivirus organization, maturation, and fusion. *Cell* **108**, 717–725 (2002).
14. Allison, S. L., Schalich, J., Stiasny, K., Mandl, C. W. & Heinz, F. X. Mutational evidence for an internal fusion peptide in flavivirus envelope protein E. *J. Virol.* **75**, 4268–4275 (2001).
15. Levy-Mintz, P. & Kielian, M. Mutagenesis of the putative fusion domain of the Semliki Forest virus spike protein. *J. Virol.* **65**, 4292–4300 (1991).
16. Ahn, A., Gibbons, D. L. & Kielian, M. The fusion peptide of Semliki Forest virus associates with sterol-rich membrane domains. *J. Virol.* **76**, 3267–3275 (2002).
17. Gibbons, D. L. *et al.* Conformational change and protein–protein interactions of the fusion protein of Semliki Forest virus. *Nature* **427**, 320–325 (2004).
18. Stiasny, K., Allison, S. L., Schalich, J. & Heinz, F. X. Membrane interactions of the tick-borne encephalitis virus fusion protein E at low pH. *J. Virol.* **76**, 3784–3790 (2002).
19. Wimley, W. C. & White, S. H. Partitioning of tryptophan side-chain analogs between water and cyclohexane. *Biochemistry* **31**, 12813–12818 (1992).
20. Allison, S. L., Stiasny, K., Stadler, K., Mandl, C. W. & Heinz, F. X. Mapping of functional elements in the stem-anchor region of tick-borne encephalitis virus envelope protein E. *J. Virol.* **73**, 5605–5612 (1999).

21. Zhang, W. *et al.* Visualization of membrane protein domains by cryo-electron microscopy of dengue virus. *Nature Struct. Biol.* **10**, 907–912 (2003).
22. Crill, W. D. & Roehrig, J. T. Monoclonal antibodies that bind to domain III of dengue virus E glycoprotein are the most efficient blockers of virus adsorption to Vero cells. *J. Virol.* **75**, 7769–7773 (2001).
23. Jennings, A. D. *et al.* Analysis of a yellow fever virus isolated from a fatal case of vaccine-associated human encephalitis. *J. Infect. Dis.* **169**, 512–518 (1994).
24. Lobigs, M. *et al.* Host cell selection of Murray Valley encephalitis virus variants altered at an RGD sequence in the envelope protein and in mouse virulence. *Virology* **176**, 587–595 (1990).
25. Holzmann, H., Heinz, F. X., Mandl, C. W., Guirakhoo, F. & Kunz, C. A single amino acid substitution in envelope protein E of tick-borne encephalitis virus leads to attenuation in the mouse model. *J. Virol.* **64**, 5156–5159 (1990).
26. Jiang, W. R., Lowe, A., Higgs, S., Reid, H. & Gould, E. A. Single amino acid codon changes detected in louping ill virus antibody-resistant mutants with reduced neurovirulence. *J. Gen. Virol.* **74**, 931–935 (1993).
27. Gao, G. F., Hussain, M. H., Reid, H. W. & Gould, E. A. Identification of naturally occurring monoclonal antibody escape variants of louping ill virus. *J. Gen. Virol.* **75**, 609–614 (1994).
28. Cecilia, D. & Gould, E. A. Nucleotide changes responsible for loss of neuroinvasiveness in Japanese encephalitis virus neutralization-resistant mutants. *Virology* **181**, 70–77 (1991).
29. Chen, Y. *et al.* Dengue virus infectivity depends on envelope protein binding to target cell heparan sulfate. *Nature Med.* **3**, 866–871 (1997).
30. Navarro-Sanchez, E. *et al.* Dendritic-cell-specific ICAM3-grabbing non-integrin is essential for the productive infection of human dendritic cells by mosquito-cell-derived dengue viruses. *EMBO Rep.* **4**, 1–6 (2003).
31. Tassanetriphep, B. *et al.* DC-SIGN (CD209) mediates dengue virus infection of human dendritic cells. *J. Exp. Med.* **197**, 823–829 (2003).
32. Stiasny, K., Allison, S. L., Marchler-Bauer, A., Kunz, C. & Heinz, F. X. Structural requirements for low-pH-induced rearrangements in the envelope glycoprotein of tick-borne encephalitis virus. *J. Virol.* **70**, 8142–8147 (1996).
33. Chan, D. C. & Kim, P. S. HIV entry and its inhibition. *Cell* **93**, 681–684 (1998).
34. Kuzmin, P. I., Zimmerberg, J., Chizmadzhev, Y. A. & Cohen, F. S. A quantitative model for membrane fusion based on low-energy intermediates. *Proc. Natl Acad. Sci. USA* **98**, 7235–7240 (2001).
35. Razinkov, V. I., Melikyan, G. B. & Cohen, F. S. Hemifusion between cells expressing hemagglutinin of influenza virus and planar membranes can precede the formation of fusion pores that subsequently fully enlarge. *Biophys. J.* **77**, 3144–3151 (1999).
36. Kozlov, M. M. & Chernomordik, L. V. A mechanism of protein-mediated fusion: coupling between refolding of the influenza hemagglutinin and lipid rearrangements. *Biophys. J.* **75**, 1384–1396 (1998).
37. Wahlberg, J. M., Bron, R., Wilschut, J. & Garoff, H. Membrane fusion of Semliki Forest virus involves homotrimers of the fusion protein. *J. Virol.* **66**, 7309–7318 (1992).
38. Han, X., Bushweller, J. H., Cafiso, D. S. & Tamm, L. K. Membrane structure and fusion-triggering conformational change of the fusion domain from influenza hemagglutinin. *Nature Struct. Biol.* **8**, 715–720 (2001).
39. Ito, H., Watanabe, S., Sanchez, A., Whitt, M. A. & Kawakoa, Y. Mutational analysis of the putative fusion domain of Ebola virus glycoprotein. *J. Virol.* **73**, 8907–8912 (1999).
40. Kemble, G. W., Danieli, T. & White, J. M. Lipid-anchored influenza hemagglutinin promotes hemifusion, not complete fusion. *Cell* **76**, 383–391 (1994).
41. Armstrong, R. T., Kushnir, A. S. & White, J. M. The transmembrane domain of influenza hemagglutinin exhibits a stringent length requirement to support the hemifusion to fusion transition. *J. Cell Biol.* **151**, 425–437 (2000).
42. Dutch, R. E. & Lamb, R. A. Deletion of the cytoplasmic tail of the fusion protein of the paramyxovirus simian virus 5 affects fusion pore enlargement. *J. Virol.* **75**, 5363–5369 (2001).
43. Baldwin, C. E., Sanders, R. W. & Berkhout, B. Inhibiting HIV-1 entry with fusion inhibitors. *Curr. Med. Chem.* **10**, 1633–1642 (2003).
44. Kilby, J. M. *et al.* Potent suppression of HIV-1 replication in humans by T-20, a peptide inhibitor of gp41-mediated virus entry. *Nature Med.* **4**, 1302–1307 (1998).
45. Hahn, Y. S. *et al.* Nucleotide sequence of dengue 2 RNA and comparison of the encoded proteins with those of other flaviviruses. *Virology* **162**, 167–180 (1988).
46. Ivy, J., Nakano, E. & Clements, D. Subunit immunogenic composition against dengue infection. US Patent 6,165,477 (1997).
47. Cuzzubbo, A. J. *et al.* Use of recombinant envelope proteins for serological diagnosis of dengue virus infection in an immunochromatographic assay. *Clin. Diagn. Lab. Immunol.* **8**, 1150–1155 (2001).
48. Otwinowski, Z. & Minor, W. Processing of X-ray diffraction data collected in oscillation mode. *Methods Enzymol.* **276**, 307–326 (1997).
49. Navaza, J. Implementation of molecular replacement in AMoRe. *Acta Crystallogr. D* **57**, 1367–1372 (2001).
50. Brünger, A. T. *et al.* Crystallography NMR system: A new software suite for macromolecular structure determination. *Acta Crystallogr. D* **54**, 905–921 (1998).
51. Jones, T. A., Zou, J. Y., Cowan, S. W. & Kjeldgaard, M. Improved methods for building protein models in electron density maps and the location of errors in these models. *Acta Crystallogr. A* **47**, 110–119 (1991).

Supplementary Information accompanies the paper on www.nature.com/nature.

Acknowledgements We thank staff at BioCARS beamline 14-BM-C at the Advanced Photon Source (Argonne National Laboratory). We thank J. Zimmerberg, F. Rey and F. Heinz for discussions, and T. Walz and Y. Cheng for guidance on EM experiments. This work was supported by a long-term fellowship to Y.M. from the Human Frontier Science Program Organization, and by an NIH grant to S.C.H., who is a Howard Hughes Medical Institute Investigator.

Competing interests statement The authors declare that they have no competing financial interests.

Correspondence and requests for materials should be addressed to S.C.H. (harrison@crystal.harvard.edu). Coordinates have been deposited in the Protein Data Bank under accession code 1OK8.